Experimental research on natural circulation characteristics of passive residual heat removal system for molten salt reactor

CHEN Kailun[1,2], YAN Changqi[1], FAN Guangming[1], MENG Zhaoming[1], and DING Tao[1]

1. *Fundamental Science on Nuclear Safety and Simulation Technology Laboratory, Harbin Engineering University, Harbin 150001, China (kailunchen@hrbeu.edu.cn, changqi_yan@163.com).*
2. *Zhejiang Electric Power Design Institute Co., Ltd., China Energy Engineering Group, Hangzhou 310012, China.*

Abstract: A full-scale passive residual heat removal system for 2 MW molten salt reactor has been designed and constructed to perform experimental studies. The present research aims at investigating the transient behaviors of natural circulation during the start-up process, as well as steady state natural circulation characteristics. It is seen that fluid within the loop remains stagnant for a long period at the beginning, and natural circulation will not initiate until boiling occurs in the heating section, which is resulted from the special structure of cooling thimble. Six cooling thimbles are used in the system. At normal operation temperature of 643℃, each cooling thimble has a heat carrying capacity of 2665 W. It is found that for heat transfer from thimble tube to bayonet tube, radiation and conduction heat transfer dominate in steady state conditions and start-up transient, respectively. In addition, for two-phase natural circulation in the cooling thimble, the correlation between mass flow rate and heat transfer rate has been analyzed.

Keywords: passive; residual heat removal; start-up; natural circulation; heat transfer

1 Introduction

Considerable amounts of decay heat will be produced by the fission products after the reactor shutdown, which must be removed in time to avoid the overheating of nuclear fuel. In recent years, it is noticed that the application of passive residual heat removal system (PRHRS) can significantly enhance the safety of nuclear power systems under accident conditions. As a result, passive cooling systems utilizing natural circulations have been widely adopted in advanced water cooled reactors [1-3]. In order to achieve the goals of high levels of safety and reliability in the Generation IV reactor designs, PRHRS is being seriously considered for its potential applications [4]. As a candidate of next generation nuclear systems, molten salt reactor (MSR) was first developed at Oak Ridge National Laboratory (ORNL) to serve as a high power density aircraft reactor [5]. Later, much work related to the Molten Salt Reactor Experiment (MSRE) [6], a 7.4 MW test reactor with nuclear fuel dissolved in fluoride salt, was done through 1960s, and the successful operation of the MSRE demonstrated the feasibility of the liquid fuel reactor. In recent years, some conceptual designs of MSR have been put forward, including the molten salt actinide recycler and transforming system (MOSART) [7], the integral molten salt reactor (IMSR) [8], and the molten salt fast reactor (MSFR) [9]. In 2011, the thorium molten salt reactor (TMSR) research project was launched by Shanghai Institute of Applied Physics and a 2 MW TMSR based on liquid fuel technology was to be constructed in a few years [10]. A unique feature of MSR is that it employs liquid fuel to circulate through the core, which makes it much easier to remove the fuel from the reactor. In any shutdown of MSR during which the reactor must be cooled, the fuel salt will be transferred from the core to a drain tank. Consequently, the PRHRS designed for water cooled reactor cannot be applicable in this case, which clearly shows the necessity of developing an innovative PRHRS for MSR.

Natural circulation systems have been widely employed in industrial applications, such as solar heat collectors, electronic equipment cooling systems and residual heat removal systems for nuclear reactors. In a work presented by Franco and Filippeschi [11], the connection between heat transfer capability and fluid dynamic performance in a two phase thermosiphon was studied experimentally.

Received date: January 5, 2018
(Revised date: October 11, 2017)

From the results, it was seen that the maximum mass flow rate varied with different working pressure, filling ratio and fluid property. Hua *et al.* [12] and Zhang *et al.* [13] performed experimental studies to investigate the thermal performance characteristics of a two-phase natural circulation system for solar collector at different heating load. It was found that the backflow phenomenon would occur at the inlet of receiver during the start-up transient of system, which could remarkably influence the total thermal resistance of the steam generation system when the heating load was not high. Kudariyawar *et al.* [14] conducted both experimental and theoretical analyses on thermal-hydraulic behaviors of a natural circulation loop using solar nitrate salt as working fluid. During the flow initiation transient, oscillations of mass flow rate and temperatures in the heating section were observed. Honda *et al.* [15] reported the flow performance of a two-phase natural circulation system with small dimension for electronic components cooling. The operation characteristics of the passive decay heat removal system of an integral reactor was evaluated by Park *et al.* [16] through experiments. From the study, it was shown that the single-phase natural circulation in the primary loop and the two-phase natural circulation in the PRHRS loop worked together to dissipate the decay heat from the core. Wang *et al.* [17] proposed a sodium heat pipe for use in the PRHRS of MSR, and numerical simulations with a two-dimension model were carried out to predict the variations of temperature, pressure and vapor flow in the start-up process. The calculation results suggested that the heat pipe reached the steady state within 400 s. As an improved version, the heat pipe using sodium-potassium alloy was also devised [18]. The behaviors of a passive cooling system for lead cooled fast reactor were analyzed by Damiani *et al.* [19] with Matlab-Simulink module, and the results indicated that the heat removal rate of the bayonet heat exchangers and isolation condenser fluctuated throughout the decay period. For all the researches mentioned above, in spite of a wide power range and a diverse set of loop structures, it is found that complicated phenomena will probably occur in natural circulation systems. Accordingly, it is necessary to investigate the heat transfer capacity and flow characteristics of natural circulation in the PRHRS.

The objective of the present research is to investigate the natural circulation characteristics and thermal performance of a PRHRS adapted to MSR. Experiments have been conducted in a full-scale drain tank passive cooling system for 2 MW MSR. The flow characteristics and associated phenomena of natural circulation in the cooling thimble during start-up process are discussed in detail. Efforts are made to obtain the heat removal rate of the system, and to analyze the connection between mass flow rate and heat transfer rate.

2 Experimentation

2.1 Description of the experimental facility

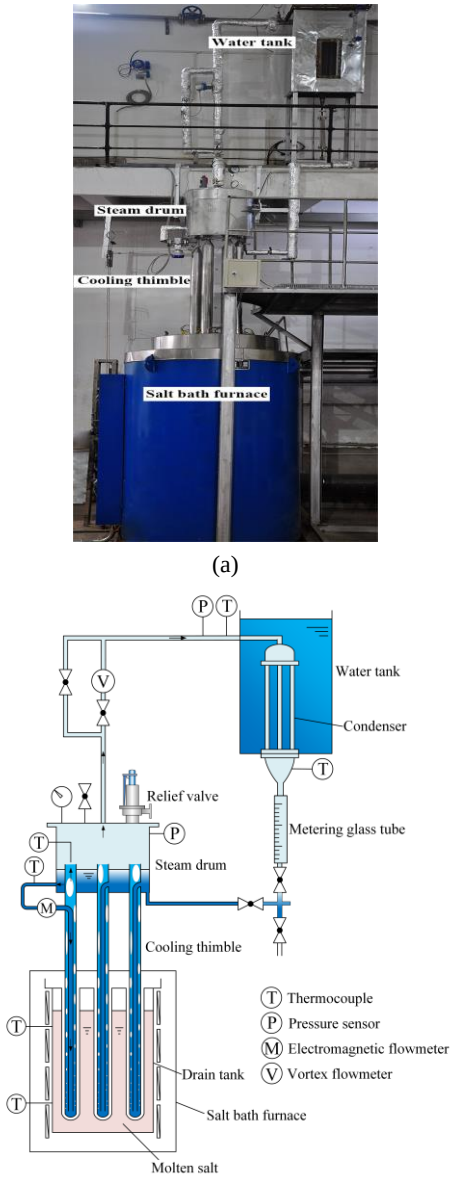

Fig. 1. Experimental facility in (a) photograph and in (b) schematic view.

Many experimental studies have been carried out with scaled-down systems and reduced power range, so that only qualitative analysis can be done. In this work, according to the results and information obtained in our previous study [20], a full-scale thimble based passive cooling facility applied to 2 MW MSR has been designed and constructed, as illustrated in Fig. 1. The experimental facility mainly consists of a high temperature salt bath furnace, six cooling thimbles, a steam drum, a water tank with an immersed condenser, some valves and connecting pipes. The salt bath furnace includes a drain tank and heating system with the maximum operation temperature of 850℃. The drain tank is 600 mm in internal diameter and 1800 mm high, and contains about 450 L salt (38 wt%Li_2CO_3-30 wt%Na_2CO_3-32 wt%K_2CO_3).

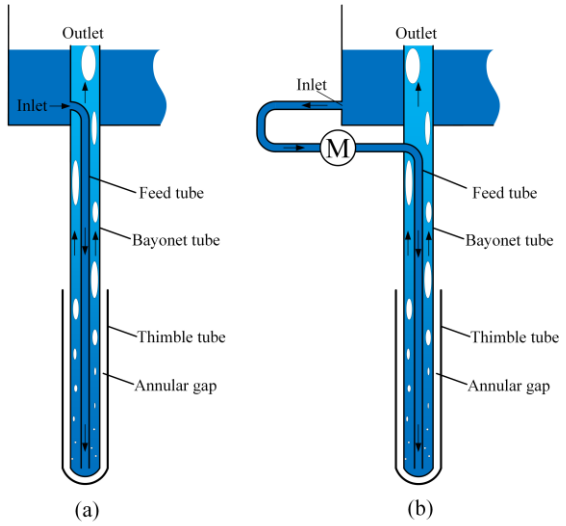

Fig. 2. Schematic diagram of cooling thimble: (a) original structure, (b) improved structure for flow rate measurement.

Six cooling thimbles extend vertically into the drain tank to remove the sensible heat from molten salt, and these cooling thimbles are evenly spaced on a circle with a diameter of 346 mm. The cooling thimble is a tube-in-tube heat exchanger with a closed bottom, and has three concentric tubes, including the thimble tube, the bayonet tube, and the feed tube, which is shown in Fig. 2(a). Water is chosen as coolant in this research. Since the contact between water and molten salt will result in an explosion due to liquid water flashing, high degree of safety must be ensured. The thimble tube wall and the bayonet tube wall act as two barriers separating molten salt from water, and the annular space between two tubes is filled with air. One design purpose of the air gap is to provide the required thermal resistance for heat transfer. Another design purpose of the proposed structure is to avoid the contact between water and molten salt even in case of a thimble tube or bayonet tube break. Water in the steam drum enters the cooling thimble from the inlet of feed tube, and is vaporized at the inner surface of bayonet tube in heating section. Consequently, natural circulation is established inside cooling thimble due to density difference between fluid in bayonet tube and feed tube. It may be noted that both the inlet and outlet of cooling thimble are in the steam drum, which makes it difficult to measure the flow rate. Thus, for one of these cooling thimbles, a short section of feed tube is deliberately designed to be outside the steam drum to allow the installation of an electromagnetic flowmeter (KROHNE OPTIFLUX 4000) which measures the inlet flow rate, as shown in Fig. 2(b). This short section has a diameter slightly larger than inner feed tube to compensate the friction loss by additional bends, so the flow characteristics of these two designs are assumed to be the same. The steam generated in bayonet tubes is separated in the steam drum, and flows upward via pipes and a vortex flowmeter (Endress+Hauser Prowirl D 200) before it is condensed in a condenser immersed in a water tank. The condenser is in the form of a vertical tube buddle fabricated of copper-nickel alloy B30. The condensate returns to steam drum by gravity. During the operation, the steam produced in water tank is directly discharged to atmosphere. Aluminum silicate fiber with 300 mm and 50 mm thick is used to insulate heat for the salt bath furnace and other components in the system, respectively. Other main parameters are listed in Table 1.

For each cooling thimble, six thermocouples of 3 mm diameter are argon arc welded on the outer surface of thimble tube, and six thermocouples of 0.5 diameter are attached on the outer surface of bayonet tube in the same relative position using silver brazing technique, as shown in Fig. 3. These thermocouples are K-type and sheathed with Inconel 600. In addition, the inlet and outlet temperatures of the cooling thimble and the condenser are monitored by four thermocouples. Pressure sensors have been placed on

the steam drum and at the condenser inlet. All the signals are collected and recorded by a data acquisition system (NI PXIe 1073, 4353, and 4300).

Table 1 Main parameters of the system.

Parameter	Value
System operation pressure	0.1-0.2 MPa
Cooling thimble	
Number	6
Thimble tube	
Diameter(OD/ID)	38.10 mm/35.10 mm
Length	1700 mm
Bayonet tube	
Diameter(OD/ID)	25.40 mm/22.40 mm
Length	3485 mm
Feed tube	
Diameter(OD/ID)	12.19 mm/9.99 mm
Length	3320 mm
Steam drum	
Diameter	500 mm
Height	500 mm
Condenser tube	
Number	9
Diameter (OD/ID)	16 mm/13 mm
Length	800 mm

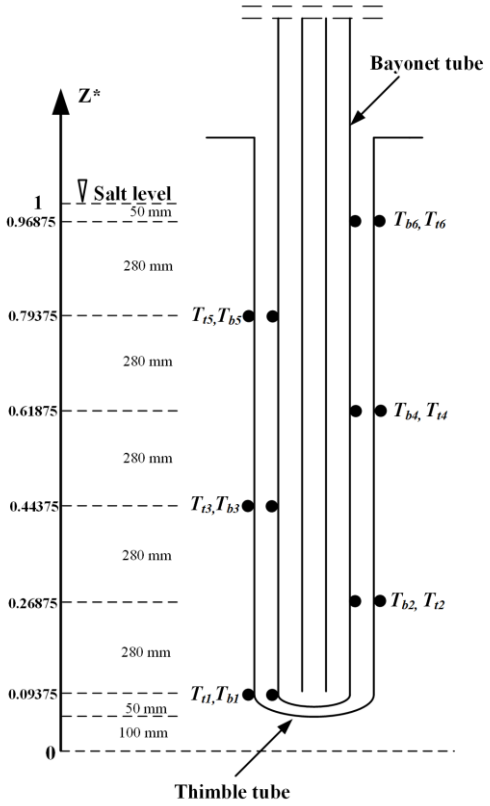

Fig. 3. Thermocouple arrangements.

2.2 Uncertainty analysis

All the thermocouples used have been calibrated individually in the working temperature range, and the accuracy are ±0.7℃ and ±0.4% of reading for temperature measurement below and above 200℃, respectively. The electromagnetic flowmeter and vortex flowmeter have measurement errors better than ±0.2% and ±1% of actual flow rate, respectively, which is proved by calibration certificates from the manufacturer. The pressure transmitters have been calibrated against a piston gauge to have accuracies within ±0.075% of reading. At steady states, the heat removal rate of the system can be calculated based on the saturated steam generation rate and latent heat of vaporization, as shown in Eq. (4). As a derived parameter, the uncertainty of heat removal rate can be computed according to the error propagation method by Moffat [21]. The latent heat of vaporization for water is considered to be a constant. Thus, the relative uncertainty of heat removal rate is the same with that of steam flow rate in the system, which is ±1%.

3 Results and discussions

3.1 Natural circulation characteristics during the start-up process

The fuel salt will be transferred to the drain tank after the reactor shutdown. If the high temperature salt comes into contact with drain tank and cooling thimbles at room temperature, the consequent thermal stresses may bring a risk of damaging structural materials. Thus, the drain tank needs to be preheated to a high temperature before liquid salt enters. In this section, this preheating process is identified as the start-up transient of the system.

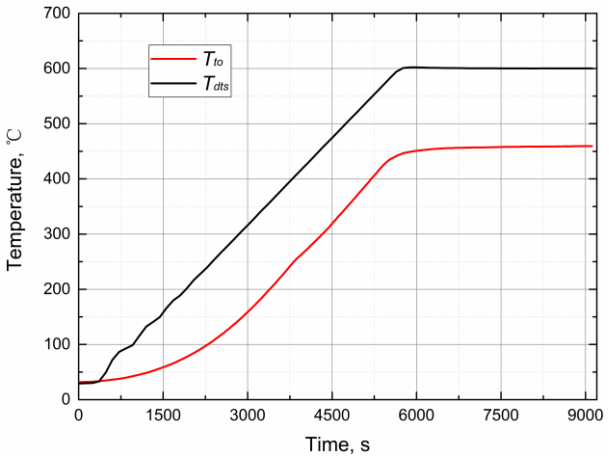

Fig. 4. Temperature variations of drain tank surface and thimble tube surface in start-up process.

The temperature variations of drain tank surface and thimble tube outer surface during the preheating

process are plotted in Fig. 4. The target temperature of drain tank surface is set to 600℃ with a heating rate of 6 ℃/min. With air in the drain tank, the temperature of thimble tube surface reaches a steady state value of 460℃, which is much lower than that of drain tank surface. Based on the transient characteristics of natural circulation flow rate in the cooling thimble presented in Fig. 5, the start-up transient of the system can be divided into four stages: (a) flow initiation, (b) single-phase natural circulation, (c) unstable two-phase natural circulation, and (d) stable two-phase natural circulation.

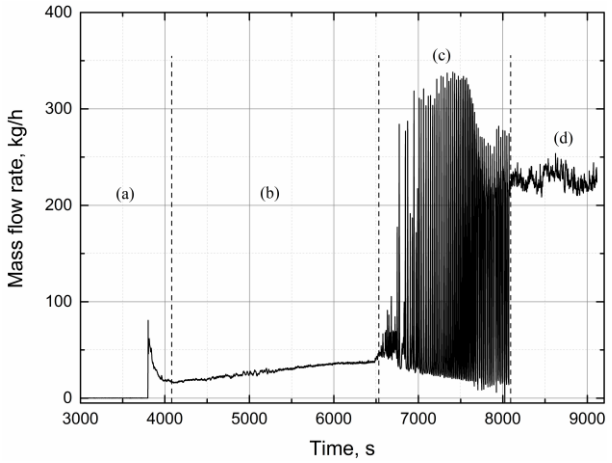

Fig. 5. Natural circulation flow rate in the cooling thimble during start-up process.

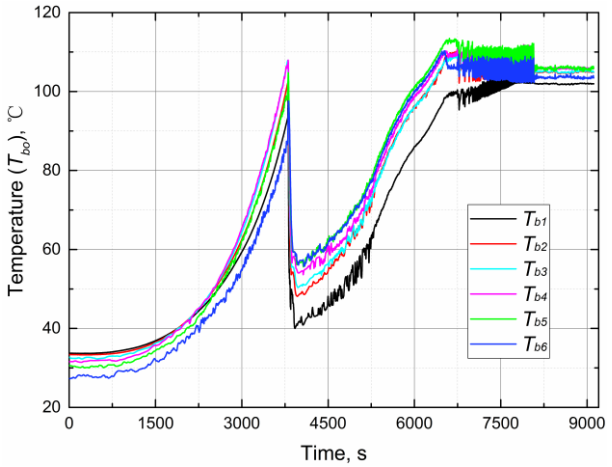

Fig. 6. Temperature variations of bayonet tube surface in start-up process.

In the flow initiation stage, the fluid within the loop remains stationary for a long period of time. Since there is no flow, the heat transferred from thimble tube to bayonet tube cannot be dissipated in time, and thus the bayonet tube temperature continues to rise as shown in Fig. 6. It is seen that T_{b3} and T_{b4} are the first to reach the saturation temperature of local fluid, which means bubble nucleation firstly occurs in the middle region of bayonet tube. Combined with results obtained from Fig. 5 and Fig. 6, temperatures of bayonet tube reach peak values at 3800 s, and a continuous flow is established in the cooling thimble simultaneously. This flow is caused by the departure of growing bubbles at heating surface, which significantly increases the density difference between fluid in downcomer and annulus riser. It is also noteworthy that there is an axial variation in the bayonet tube temperature, and T_{b1} and T_{b6} are relatively low with no boiling when flow begins. The flow promotes bubble departure in the heating section, which will further increase the driving force and flow rate of natural circulation, and it only takes 3 s for the flow rate to peak. As a result, the wall temperature of bayonet tube declines sharply due to enhanced heat transfer, and no bubble can be generated on the heating surface. After the annulus riser is filled with cold water, the flow rate keeps dropping because of decreased driving force, and single-phase natural circulation stage is attained. In this stage, the heat is carried away by steady single-phase flow. Moreover, the wall temperature of bayonet tube gradually increases along the flow direction.

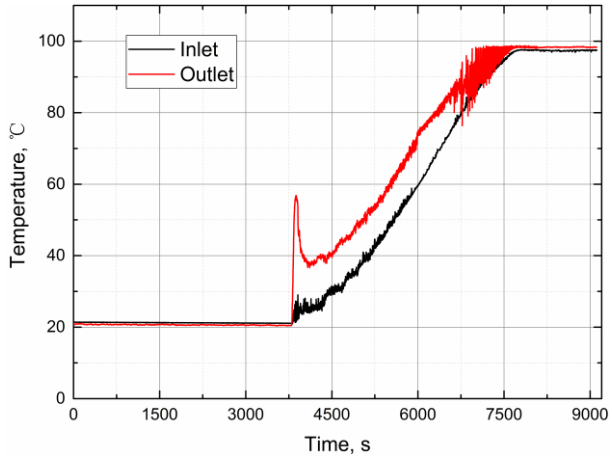

Fig. 7. Inlet and outlet temperature variations of cooling thimble in start-up process.

It can be seen from Fig. 7 that the outlet temperature of cooling thimble increases rapidly when natural circulation initiates. In fact, the fluid temperature at the outlet of heating section is near saturation point at this moment. However, the circulating fluid will be cooled by cold water in the down comer as it passes through the annulus riser. Therefore, the maximum outlet temperature of cooling thimble during flow initiation is 57℃. As shown in Fig. 5 and Fig. 7, the

flow rate of single-phase natural circulation increases from 16 kg/h to 38 kg/h with the increasing inlet temperature. The fluid temperature and bayonet tube temperature keep rising as heat is continuously absorbed, and the two-phase natural circulation occurs again at 6490 s. The flow rate oscillates with large amplitude when the inlet temperature varies from 73.3℃ to 97.5℃. This kind of flow instability was also observed in our previous study at low boundary temperature condition, which was identified as flashing-induced density wave oscillation [22]. When saturated fluid enters the riser and flows upward, it will become overheated due to reduced static head, and a part of the fluid will flash into vapor. Meanwhile, flash evaporation dramatically increases the driving force and the flow rate in the loop. Then, with the intensified heat transfer, the wall temperature of bayonet tube and fluid temperature in the riser both decrease, which results in the disappearance of flashing. The flow rate becomes relatively low, and the fluid temperature in heating section continues to climb until the flashing phenomenon happens again. It must be noticed that when the inlet temperature exceeds 97.5℃, the two-phase natural circulation becomes stable. In this stage, flashing has a slight influence on the void fraction in the riser, and thus the flow rate oscillation is not pronounced. These results indicate that if the inlet temperature is maintained near its saturation point, flow instabilities can be avoided in the start-up process of the system.

The start-up process of natural circulation in cooling thimble is quite different from that in common natural circulation loop having isolated down comer and riser, in which single-phase fluids start to circulate shortly after heating begins. For the cooling thimble, a unique characteristic is that the fluid in the loop keeps stagnant after heating for a long time (from 0 to 3800 s). In addition, the system will not directly enter single-phase natural circulation state until the temperature on bayonet tube wall reaches the saturation point of local fluid and a short period of two-phase natural circulation happens. Thus, it can also be deemed as the single-phase natural circulation caused by two-phase natural circulation. The possible causes accounting for the phenomenon above include: (1) the fluid remains still at first; when the fluid in heating section is heated, the fluid in down comer exchanges heat with that in heating section through the tube wall so that they do not differ very much in respect of temperature and density and the driving force is insufficient to balance the resistance along the loop and then produce single-phase natural circulation flow; therefore, the fluid remains stagnant for a long period due to the special structure of cooling thimble; (2) before the flow starts, only the fluid in heating section has relatively high temperature whereas fluid in riser has low temperature, so the total driving force in the loop is far from being high; after two-phase flow begins, the fluid temperature in riser increases prominently. Although the fluid in heating section stops boiling shortly after, and the fluid in the loop returns to the single-phase state, the fluid temperature in both heating section and riser remains being relatively high, and hence single-phase natural circulation can be maintained with the corresponding driving force.

The heat transferred from thimble tube to bayonet tube mainly includes two parts, thermal radiation and conduction. The radiation heat removal rate can be expressed as:

$$Q_r = \frac{\sigma\left(T_{ti}^4 - T_{bo}^4\right)}{\frac{1-\varepsilon_{bo}}{\varepsilon_{bo}A_{bo}} + \frac{1}{A_{bo}X_{bo,ti}} + \frac{1-\varepsilon_{ti}}{\varepsilon_{ti}A_{ti}}} \tag{1}$$

where T_{ti} is inner wall temperature of thimble tube and T_{bo} is outer wall temperature of bayonet tube. ε represents the total emissivity for radiating and receiving surface. A is the heat exchange area and $X_{bo,ti}$ is the angle factor, which equals to 1 in this condition.

The conduction heat transfer rate through the air gap can be calculated by Eq. (2).

$$Q_c = \frac{2\pi\lambda_{ag}L\left(T_{ti} - T_{bo}\right)}{\ln\left(D_{ti}/D_{bo}\right)} \tag{2}$$

where λ_{ag} is the thermal conductivity of the air gap, and L is the length of heating section.

The total heat transfer rate of the cooling thimble is determined by the formula.

$$Q_{total} = Q_r + Q_c \tag{3}$$

Under the quasi-steady-state assumption, the heat transfer rate of one cooling thimble during start-up process can be calculated by Eqs. (1) -(3). The variations of heat transfer rate with time are depicted in Fig. 8. During the first 3000 s, radiation heat

transfer rate is quite small because of the low surface temperature of thimble tube, and conduction heat transfer rate accounts for more than 87% of the total heat transfer rate. It is noted that the increase in conduction heat transfer rate speeds up when flow initiates. The reason for this variation is that the bayonet tube temperature decreases rapidly with elevated flow rate, which dramatically increases the temperature difference between the thimble and bayonet tube. However, this increase in temperature difference caused by flow initiation slightly influences the radiation heat transfer rate. After about 6000 s, the total heat transfer rate is almost constant, and a steady state value of 730 W is finally attained. As the driving temperature difference is increased gradually, the contribution of thermal radiation is raised to 32%. Overall, conduction heat transfer plays a dominant role in the start-up process. Besides, although flow instability may result in temperature oscillations of bayonet tube, it has little effect on either conduction or radiation heat transfer rate.

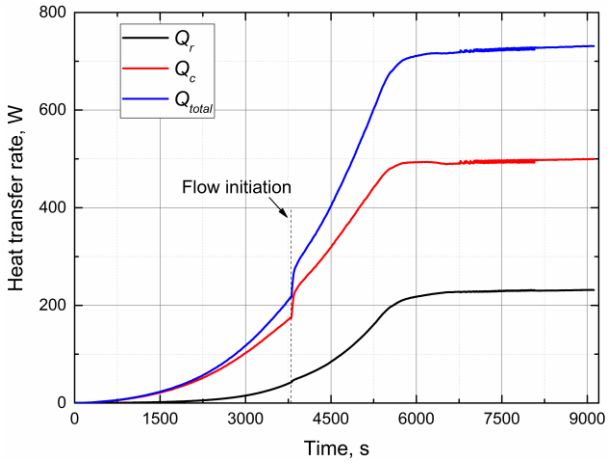

Fig. 8. Variations of heat transfer rate for one cooling thimble in start-up process.

3.2 Natural circulation characteristics at steady states

In this section, analysis has been made to study the heat transfer and flow capability of natural circulation inside the cooling thimble at steady states. The drain tank is filled with carbonate salt instead of the fuel salt. Fluid in the steam dome and condensation tank is saturated during the test.

3.2.1 Heat transfer capability

The influence of the boundary temperature on the heat removal capability of the passive cooling system is shown in Fig. 9. The radiation heat transfer rate Q_r from thimble tube to bayonet tube can be calculated by Eq. (1). It should be mentioned that the system has six cooling thimbles inserted into the molten salt for residual heat removal. In order to analyze the thermal performance of one cooling thimble, the heat transfer rate shown in Fig. 9 is one-sixth of the overall heat transfer rate of the system, which can be calculated based on the steam generation rate and latent heat of evaporation as

$$Q = M \times h_{fg} \tag{4}$$

T_{to} represents the mean temperature reading of thermocouples mounted on the outer wall of thimble tube, which is in contact with the molten salt. At a high molten salt temperature of 643℃, each cooling thimble has the heat transport capability (Q) of 2665 W. It is observed that the variations in heat transfer rate are significant at high salt temperatures. With the decreasing boundary temperature, the decrease in total heat transfer rate slows continuously. At boundary temperature of 405℃, which is slightly below the solidifying point of molten salt, the cooling thimble demonstrates heat removal capability of 842 W. The heat transfer rate stays at a relatively low level after the salt is completely frozen. Accordingly, the passive cooling system would be able to maintain salt temperature within safety limits, as well as keep the molten salt from solidifying for a long time during the decay period.

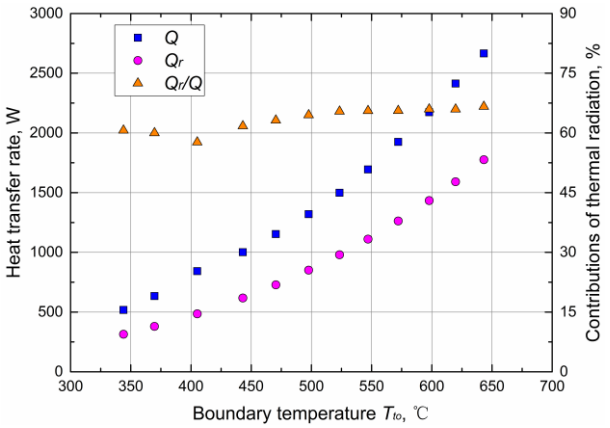

Fig. 9. Heat removal capability of one cooling thimble at different boundary temperature.

Since heat transfer medium (air) exists between the thimble tube and the bayonet tube, radiation, conduction and convection heat transfer are assumed to proceed at the same time. For natural convection in the annular gap, the Grashof number Gr can be expressed as

$$Gr = \frac{g\beta\left(T_{ti} - T_{bo}\right)\delta^3}{\nu^2} \quad (5)$$

The maximum value of *Gr* is 233 in the whole test range, so that convection heat transfer can be neglected in the following analysis. The radiation heat transfer rate Q_r from thimble tube to bayonet tube can be calculated by Eq. (1), and the variation of Q_r, corresponding to the variation of the total heat transfer rate, is also shown. Hastelloy C-276 is selected as the material for cooling thimbles, and the total emissivity values for radiating surface and receiving surface were measured in the Institute of Automatic Detecting and Process Control System at Harbin Institute of Technology. It is seen that radiation heat transfer rate reaches 1775 W and accounts for around 67% of the overall heat transfer rate at the salt temperature of 643℃, which indicates that thermal radiation plays a dominating role in the annular gap at high temperature. As the molten salt temperature is decreased gradually, the contribution of radiation heat transfer becomes less pronounced. At boundary temperature of 405℃, only 58% of the total heat transfer rate is being transferred by thermal radiation. It is concluded that thermal radiation prevails in heat transfer between the thimble tube and the bayonet tube over most of the normal operation temperature range, which is different from that in the start-up transition.

3.2.2 Flow capability

The mass flow rate of two-phase natural circulation in one cooling thimble at various heat transfer rate is depicted in Fig. 10. The values of heat transfer rate are obtained at different operation temperatures. It has been noted that the flow rate increases with elevated heat transfer rate. When the heat transfer rate is increased from 842 W to 1924 W, the circulation flow rate increases rapidly. Meanwhile, the slope of flow rate curve has a decreasing tendency. At higher heat transfer rate above 1924 W, the raise in heat transfer rate has little influence on mass flow rate. This is because the void fraction in the riser stays at a high level at this time; the continuous increase in heat input slightly enhances the driving force in the loop, but it will result in a remarkable rise in the flow resistance, and hence the flow rate shows little variation.

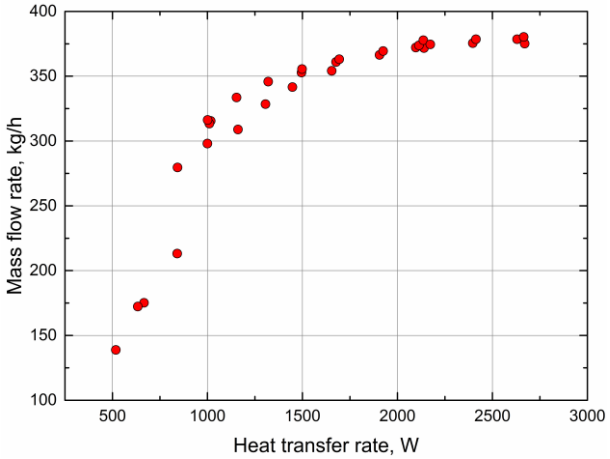

Fig. 10 Mass flow rate of natural circulation in one cooling thimble at different values of heat input.

It is worth noting that the average mass flow rate dramatically decreases when the heat transfer rate is below 842 W. This is correlated with the periodic flow oscillations which occur at low heating power, as shown in Fig. 11. The unstable flow is accompanied by periodic variations in pressure drop and vapor generation in the loop, and the flow characteristics are distinctly different from those in steady state flow.

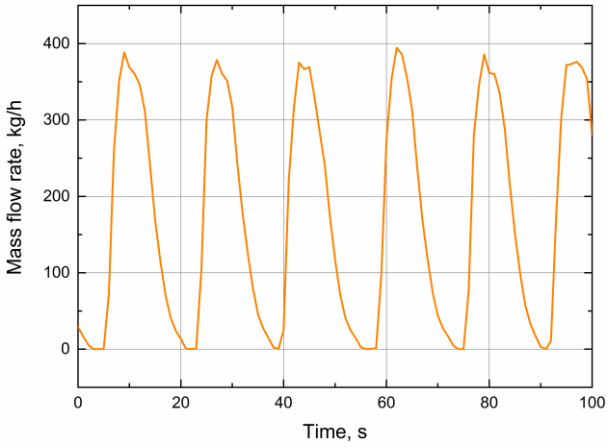

Fig. 11 Time evolution of mass flow rate in the cooling thimble for *Q* = 633 W.

4 Conclusions

In this research, the natural circulation characteristics of a full-scale passive residual heat removal facility for 2 MW molten salt reactor have been experimentally investigated. The results provide useful knowledge to understand the thermal-hydraulic behaviors and reference data for engineering applications. The main conclusions can be summarized as follows.

1) The start-up process can be divided into four stages: flow initiation, single-phase natural circulation, unstable and stable two-phase

natural circulation. In the first 3800 s, the fluid in cooling thimble remains stagnant. Single-phase natural circulation will not be established until boiling takes place at the inner surface of the bayonet tube and a short period of two-phase flow happens. These phenomena are resulted from the heat exchange between fluid in down comer and in heating section, which makes the start-up transient quite different from that in common natural circulation loops.

2) In the start-up process, the heat removal rate of the system is relatively low, which is less than 4.4 kW, and conduction heat transfer play a dominant role between thimble tube and bayonet tube. In normal operation temperature range, the passive cooling system has a heat transport capacity of 16 kW at salt temperature of 643℃, and thermal radiation dominates the heat transfer from thimble tube to bayonet tube.

3) At steady state conditions, it is found that the mass flow rate in the cooling thimble increases rapidly with the increasing heat transfer rate from 842 W to 1924 W. Higher heat transfer rate has little influence on the mass flow rate. As the periodic flow oscillations take place at low heating power, the average flow rate decreases significantly.

Nomenclature

A surface area, m^2
D diameter, m
g gravitational acceleration, m/s^2
Gr Grashof number
h_{fg} latent heat of evaporation, J/kg
ID inner diameter
L length, m
M mass flow rate of vapor, kg/s
OD outer diameter
Q heat transfer rate, W
T temperature, ℃
X angle factor
β thermal expansion coefficient, 1/℃
δ width of air gap, m
ε emissivity
λ thermal conductivity, W/(m·℃)
v kinematic viscosity, m^2/s
σ Stefan-Boltzmann constant, $W/(m^2 K^4)$

Subscripts

ag air gap
b bayonet tube
bo bayonet outer
c conduction
dts drain tank surface
r radiation
t thimble tube
ti thimble inner
to thimble outer

Acknowledgments

This work was supported by the National Natural Science Foundation of China under Grant No. 11475048.

References

[1] SCHULZ, T.L.: Westinghouse AP1000 advanced passive plant, Nucl. Eng. Des., 2006, 236(14):1547-1557.

[2] STOSIC, Z.V., BRETTSCHUH, W., and STOLL, U.: Boiling water reactor with innovative safety concept: The Generation III+ SWR-1000, Nucl. Eng. Des., 2008, 238(8):1863-1901.

[3] HINDS, D., and MASLAK, C.: Next-generation nuclear energy: The ESBWR, Nuclear News, 2006, 49(1):35-40.

[4] DOE, U.S.: A technology roadmap for generation IV nuclear energy systems, In Nuclear Energy Research Advisory Committee and the Generation IV International Forum, 2002.

[5] BETTIS, E.S., SCHROEDER, R.W., CRISTY, G.A., SAVAGE, H.W., AFFEL, R.G., and HEMPHILL, L.F.: The aircraft reactor experiment—design and construction, Nucl. Sci. Eng., 1957, 2(6):804-825.

[6] HAUBENREICH, P.N., and ENGEL, J.R.: Experience with the molten-salt reactor experiment, Nucl. Technol., 1970, 8(2):118-136.

[7] IGNATIEV, V., FEYNBERG, O., GNIDOI, I., MERZLYAKOV, A., SURENKOV, A., and UGLOV, V., *et al.*: Molten salt actinide recycler and transforming system without and with Th–U support: Fuel cycle flexibility and key material properties, Ann. Nucl. Energy, 2014, 64:408-420.

[8] LEBLANC, D.: The Integral Molten Salt Reactor (IMSR), Canadian Nuclear Society Bulletin, 2014, 35(4):28-34.

[9] HEUER, D., MERLE-LUCOTTE, E., ALLIBERT, M., BROVCHENKO, M., GHETTA, V., and RUBIOLO, P.: Towards the thorium fuel cycle with molten salt fast reactors, Ann. Nucl. Energy, 2014, 64:421-429.

[10] JIANG, M.H., XU, H.J., and DAI, Z.M.: Advanced fission energy program-TMSR nuclear energy system, Bulletin of Chinese Academy of Sciences, 2012, 27(3):366-374.

[11] FRANCO, A., and FILIPPESCHI, S.: Experimental analysis of closed loop two phase thermosyphon (CLTPT) for energy systems, Exp. Therm. Fluid Sci., 2013, 51:302-311.

[12] HUA, M., ZHANG, L., FAN, L., LV, Y., LU, H., YU, Z., and CEN, K.: Experimental investigation of effect of heat load on thermal performance of natural circulation steam generation system as applied to PTC-based solar system, Energy Convers. Manage., 2015, 91:101-109.

[13] ZHANG, L., FAN, L., HUA, M., ZHU, Z., WU, Y., and YU, Z., *et al*.: An indoor experimental investigation of the thermal performance of a TPLT-based natural circulation steam generator as applied to PTC systems, Appl. Therm. Eng., 2014, 62(2):330-340.

[14] KUDARIYAWAR, J.Y., SRIVASTAVA, A.K., VAIDYA, A.M., MAHESHWARI, N.K., and SATYAMURTHY, P.: Computational and experimental investigation of steady state and transient characteristics of molten salt natural circulation loop, Appl. Therm. Eng., 2016, 99:560-571.

[15] HONDA, H., ZHANG, Z., and TAKATA, N.: Flow and heat transfer characteristics of a natural circulation evaporative cooling system for electronic components, J. Electron. Packag., 2004, 126(3):317-324.

[16] PARK, H.S., CHOI, K.Y., CHO, S., YI, S.J., PARK, C.K., and CHUNG, M.K.: Experimental study on the natural circulation of a passive residual heat removal system for an integral reactor following a safety related event, Ann. Nucl. Energy, 2008, 35(12):2249-2258.

[17] WANG, C., ZHANG, D., QIU, S., TIAN, W., WU, Y., and SU, G.: Study on the characteristics of the sodium heat pipe in passive residual heat removal system of molten salt reactor, Nucl. Eng. Des., 2013, 265:691-700.

[18] WANG, C., GUO, Z., ZHANG, D., QIU, S., TIAN, W., WU, Y., and SU, G.: Transient behavior of the sodium–potassium alloy heat pipe in passive residual heat removal system of molten salt reactor, Prog. Nucl. Energy, 2013, 68:142-152.

[19] DAMIANI, L., GIRIBONE, P., REVETRIA, R., and PRATO, A.P.: A passive decay heat removal system for the lead cooled fast reactor demonstrator “Alfred”, Prog. Nucl. Energy, 2015, 83:294-304.

[20] CHEN, K., YAN, C., MENG, Z., WU, X., SONG, S., YANG, Z., and YU, J.: Experimental analysis on passive residual heat removal in molten salt reactor using single cooling thimble test system, Energy, 2016, 112:1049-1059.

[21] MOFFAT, R.J.: Describing the uncertainties in experimental results, Exp. Therm. Fluid Sci., 1988, 1(1):3-17.

[22] FUKUDA, K., and KOBORI, T.: Classification of two-phase flow instability by density wave oscillation model, J. Nucl. Sci. Technol., 1979, 16(2):95-108.